



Three-Dimensional Imaging and Quantitative Analysis of Blood Vessel Distribution in The Meniscus of Transgenic Mouse after Tissue Clearing

Huaxuan Sheng, M.D.^{1#}, Mingru Huang, M.D.^{1#}, Huizhu Li, M.D.^{1#}, Luyi Sun, M.D.¹, Sijia Feng, M.D.¹, Xiner Du, M.Sc.¹, Yicong Wang, Ph.D.^{2,3}, Xiaoyu Tong, M.Sc.^{2,3}, Yi Feng, M.D., Ph.D.^{2,3}, Jun Chen, Ph.D.^{1*} , Yunxia Li, M.D.^{1*} 

1. Sports Medicine Institute of Fudan University, Department of Sports Medicine, Huashan Hospital, Fudan University, Shanghai, China
2. Department of Integrative Medicine and Neurobiology, School of Basic Medical Sciences, Institutes of Brain Science, Brain Science Collaborative Innovation Centre, State Key Laboratory of Medical Neurobiology, Institute of Acupuncture and Moxibustion, Fudan Institutes of Integrative Medicine, Fudan University, Shanghai, China
3. China Shanghai Key Laboratory of Acupuncture Mechanism and Acupoint Function, Shanghai, China

Abstract

Objective: Blood supply to the meniscus determines its recovery and is a reference for treatment planning. This study aimed to apply tissue clearing and three-dimensional (3D) imaging in exploring the quantitative distribution of blood vessels in the mouse meniscus.

Materials and Methods: In this experimental study, tissue clearing was performed to treat the bilateral knee joints of transgenic mice with fluorescent vascular endothelial cells. Images were acquired using a light sheet microscope and the vascular endothelial cells in the meniscus was analysed using 3D imaging. Quantitative methods were employed to further analyse the blood vessel distribution in the mouse meniscus.

Results: The traditional three-equal-width division of the meniscus is as follows: the outer one-third is the red-red zone (RR), the inner one-third is the white-white zone (WW), and the transition area is the red-white zone (RW). The division revealed significant signal differences between the RW and WW ($P < 0.05$) zones, but no significant differences between the RR and RW zones, which indicated that the division might not accurately reflect the blood supply of the meniscus. According to the modified division (4:2:1) in which significant differences were ensured between the adjacent zones, we observed that the width ratio of each zone was $38 \pm 1\%$ (RR), $24 \pm 1\%$ (RW), and $38 \pm 2\%$ (WW). Furthermore, the blood supply to each region was verified. The anterior region had the most abundant blood supply. The fluorescence count in the anterior region was significantly higher than in the central and posterior regions ($P < 0.05$). The blood supply of the medial meniscus was superior to the lateral meniscus ($P < 0.05$).

Conclusion: Analysis of the blood supply to the mouse meniscus under tissue clearing and 3D imaging reflect quantitative blood vessel distribution, which would facilitate future evaluations of the human meniscus and provide more anatomical references for clinicians.

Keywords: Blood Supply, Fluorescence Imaging, Meniscus, Regional Anatomy, 3D Imaging

Citation: Sheng H, Huang M, Li H, Sun L, Feng S, Du X, Wang Y, Tong X, Feng Y, Chen J, Li Y. Three-dimensional imaging and quantitative analysis of blood vessel distribution in the meniscus of transgenic mouse after tissue clearing. *Cell J.* 2023; 25(8): 570-578. doi: 10.22074/CELLJ.2023.1988973.1220
This open-access article has been published under the terms of the Creative Commons Attribution Non-Commercial 3.0 (CC BY-NC 3.0).

Introduction

The meniscus consists of two wedge-shaped fibrocartilage discs located in the medial and lateral spaces between the femoral condyle and the tibial plateau of the knee joint, covering the tibial plateau. Its main functions are to conduct load, absorb shock, and maintain joint stability (1, 2). In the general population, approximately 6% of acutely injured knees sustain a meniscus repair (3). Blood supply to the meniscus is a key factor in healing after an injury (4-6). Owing to the limited blood supply of the peripheral structures, the meniscus is a relatively avascular structure supplied by the medial and lateral

genicular arteries. These arteries are the branches of the popliteal artery, which enter the meniscus at its periphery and spread radially toward its centre, and provide major vascularization to the inferior and superior aspects of each meniscus (7, 8). Traditionally, the meniscus is divided into three zones of equal width (three-equal-width) based on qualitative observation and general description. The outer one-third of the meniscus is the red-red zone (RR), the inner one-third is the white-white zone (WW), and the transition area between the RR and WW zones is the red-white zone (RW) (9-11). However, there is a lack of quantitative research on the blood supply to the meniscus.

Received: 01/February/2023, Revised: 01/May/2023, Accepted: 08/May/2023

#These authors contributed equally in this study.

*Corresponding Address: Sports Medicine Institute of Fudan University, Department of Sports Medicine, Huashan Hospital, Fudan University, Shanghai, China

Emails: biochenjun@fudan.edu.cn, liyunxia912@aliyun.com



Royan Institute
Cell Journal (Yakhteh)

Different locations of meniscal lesions correspond to various treatment strategies, including surgical and non-surgical therapies. For example, injuries in the RR zone are usually treated with meniscal repairs, whereas injuries in the WW zone require meniscectomies and have high failure rates (12). Although meniscectomy is still an option for injuries in the WW and RW zones, there is a growing consensus in favour of nonoperative therapy or meniscal repair (13-15). Moreover, successful outcomes in patients treated with physiotherapies and biological agents, such as fibrin glue, fibrin clots, platelet-rich plasma, and stem cells, suggest that the WW zone may also have a substantial blood supply (16-18). In order to guide the selection and promote the development of meniscal treatments, it is necessary to conduct more thorough and accurate research on the blood supply to the meniscus by using the most advanced technology.

Tissue clearing is an innovative technology used to study the three-dimensional (3D) structure of organisms. Unlike conventional methods, such as histopathologic examinations, tissue clearing can preserve the microscopic characteristics of the tissue. After clearing the tissue, computer software displays the 3D structure and spatial distribution of the microstructures, including vascular endothelial cells. Currently, this technique is employed for imaging of bones, teeth, and other hard tissues, and it enables innovative 3D imaging of the meniscus and quantitative analysis of its blood supply (19). This study is the first to apply both tissue clearing and 3D imaging to investigate the blood supply in the mouse meniscus.

In this study, transgenic mice were used because their vascular endothelial cells fluoresce red upon exposure to specific laser irradiation after induction. Transgenic mice display vascular endothelial cells more accurately with higher sensitivity than traditional methods such as antibody staining and ink staining. Therefore, in order to better understand the precise vascular anatomy of the meniscus, the combination of tissue clearing and 3D imaging in transgenic mice could provide quantitative analysis of the distribution of blood vessels in the meniscus. Quantitative analysis of the blood supply to the mouse meniscus could have implications for understanding the blood supply to the human meniscus. Thus, it has clinical relevance and aids clinical decision-making in adopting optimal therapies for meniscal injury (20-22).

Materials and Methods

Animal model

Three healthy, six-month-old transgenic male mice (34-40 g, Tie2-Gt(ROSA) 26Sor^{tm14} (CAG-tdTomato) Hze, 002856) were purchased from The Jackson Laboratory (SH) (Shanghai-China). The Housing conditions were natural light, temperature 21-23, 40-60% humidity, ad libitum feeding, and without specific motion training. The vascular endothelial cells of all transgenic mice were induced to emit red fluorescence by daily intraperitoneal injections of 100 μ L tamoxifen (Sigma, USA) at a concentration of 20 mg/mL [the solvent was a 1:9 mixture of anhydrous

ethanol (China McLean) and corn oil (Sigma, USA)] for seven days. After the seven-day induction, all mice were subjected to perfusion sampling. Each transgenic mouse was anesthetized by an intraperitoneal injection of 2% pentobarbital sodium solution (30 mg/kg), and the sternum was fixed under deep anaesthesia. The sternal cavity was opened near the xiphoid process at the lower end of the sternum using surgical scissors, and the heart was fully exposed. The left ventricle was rapidly perfused with 50 mL precooled (4°C) phosphate buffered saline (PBS, China Biosharp) that contained 10 U/mL heparin sodium (China Biosharp) in a perfusion needle, and the right atrial appendage was cut. The lower limbs of the animals quivered slightly after the use of 20-30 mL of 4% paraformaldehyde (China McLean), precooled at 4°C, and the increased stiffness of the animal's body after perfusion indicated a successful perfusion. After perfusion, the attached muscles around the joints were removed and the bilateral knee joints were harvested and fixed in 4% paraformaldehyde at 4°C for seven days. There were six menisci in total.

Study design

This study was approved by the Animal Ethics Committee of the Fudan University (Shanghai, China), and the animals were treated according to the approved experimental protocols (202212009Z). The bilateral knee joints of all mice were treated using a tissue clearing technique, followed by imaging studies using a light sheet fluorescence microscope. After all the knees were 3D imaged, data on the mouse meniscus and detailed parameters of the meniscus were obtained. Finally, according to the count of the vascular endothelial cell signals in the meniscus, all data were analysed using Imaris 9.8.0 (Oxford Instruments, Abingdon, UK) to quantitatively describe and summarise the blood supply of the menisci.

Tissue clearing

Polyethylene glycol (PEG) combined with a Poly (Ethylene Glycol)-Associated Solvent System (PEGASOS) for tissue clearing can be used for imaging of bones, teeth, the brain, muscles, and other tissues (23). PEGASOS was chosen after taking into consideration the thickness of the sample, higher calcium content, and hardness of the knee joint compared to other tissues. The steps in PEGASOS include clearing fluid changes, decalcification, washing of samples, decolorization, gradient tB degreasing, dehydration, transparency, and preservation (Fig.1). The knee joints of all the mice were imaged using LS18 light-sheet microscope (Nuohai Life Science, China) located at the university. All knee joints were fixed on a carrier table with silica gel, and the imaging chamber was filled with sufficient imaging solution (equal refractive index BB-PEG) for imaging under an optical microscope. A 4 \times magnification was selected for the imaging system, and the movement and focus of the flat light film on the X, Y, and Z axes were adjusted to determine the preservation of the parameters of the intact mouse knee joint imaging range. After checking the unilateral excitation light, the laser channel was

selected based on the type of autofluorescence of the transgenic mouse. Then, a 10% overlap was selected according to the experimental requirements and sample size before scanning. After scanning, the images of each knee joint were first combined using a software program, and then the combined files were transformed into an IMS format by the Imaris Converter. Imaris Stitcher software was used according to the actual situation of the tissue samples. Finally, the obtained images were analysed using Imaris 9.8.0.

Three-dimensional imaging and quantitative analysis of mouse meniscus

The surface function of Imaris 9.8.0 was used to identify the edge of the meniscus in the 3D images of the knee joint and to subsequently outline the meniscus (Fig.1). The red fluorescence signal that represented vascular endothelial cells in the meniscus was identified and collected using the Spot function. The signals of each meniscus were collected and analysed thrice to ensure the stability of the results. All fluorescence counts were considered skewed based on data features.

Log transformation ($\log_2 N$), was used to deal with the skewed fluorescence count data from the outer edge of the meniscus to the inner edge to ensure a significant difference among the three zones based on the results of our study. The skewed data were divided into three equal parts (1:1:1) in log transformation ($\log_2 N$), which aimed to divide the meniscus into three zones based on the traditional division. Considering that the lowest value was 2, the actual ratio was calculated to be 4:2:1 (24, 25). Based on the fluorescence count collected by the software, the distribution of blood vessels on the meniscus was analysed as follows: i. A comparison of the traditional three-equal-width division with the modified division based on 3D imaging and quantitative analysis and ii. Observation of the difference in blood vessels according to the anterior, body, and posterior regions iii. Observation of the difference in blood vessels according to the medial and lateral meniscus (5). The photo and video functions of Imaris 9.8.0 were used to capture and film the fluorescence signals of the meniscus vascular endothelial cells and the overall 3D contours (Fig.2, Supplementary Video 1, See Supplementary Online Information at www.celljournal.org).

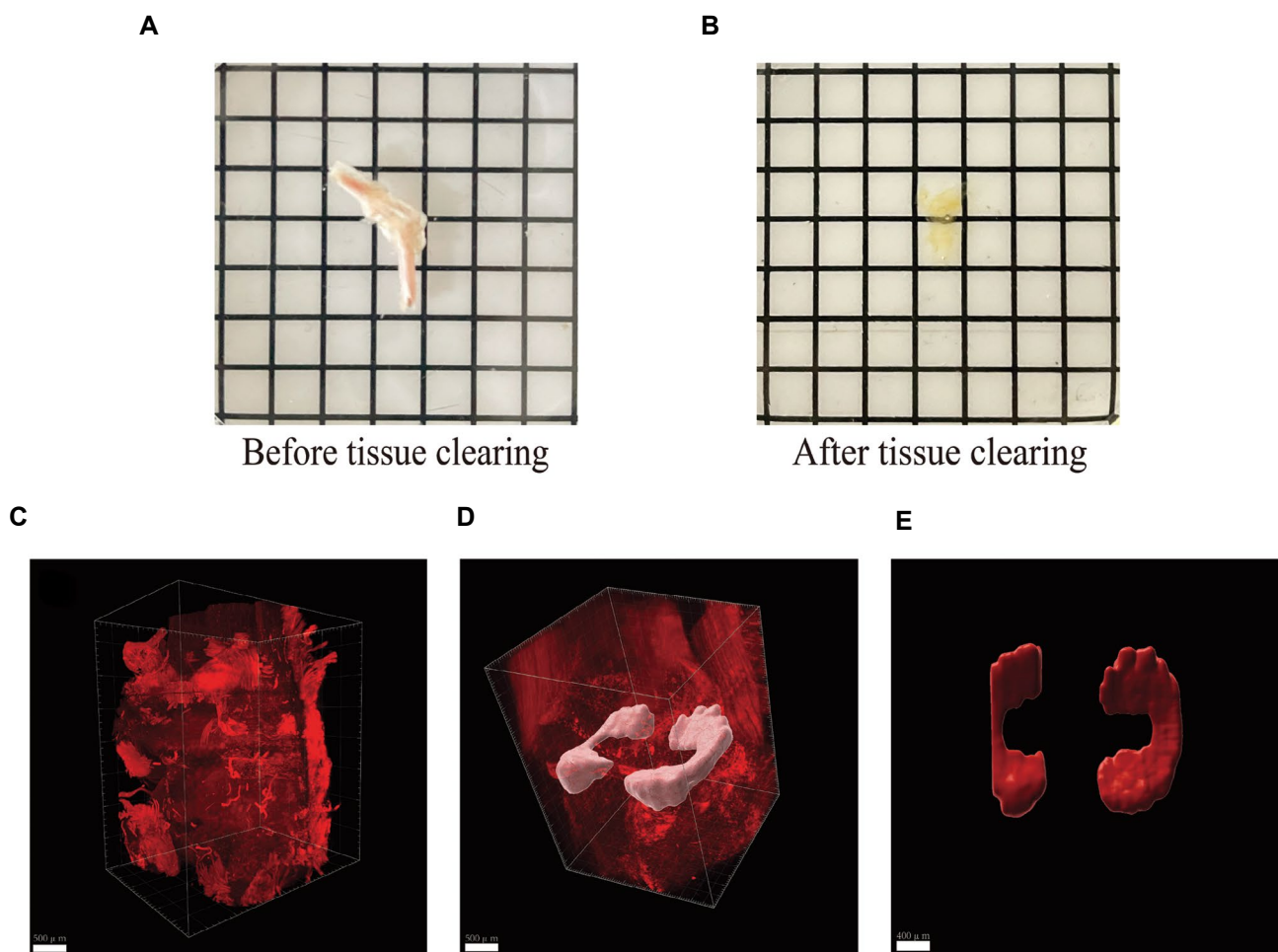


Fig.1: The brightfield images of mouse knee joint before and after tissue clearing and three-dimensional (3D) imaging of mouse meniscus. **A.** Before tissue clearing. **B.** After clearing. **C.** Mouse knee joint (scale bar: 500 μm). **D.** Mouse knee joint and meniscus (scale bar: 500 μm). **E.** Mouse meniscus (scale bar: 400 μm).

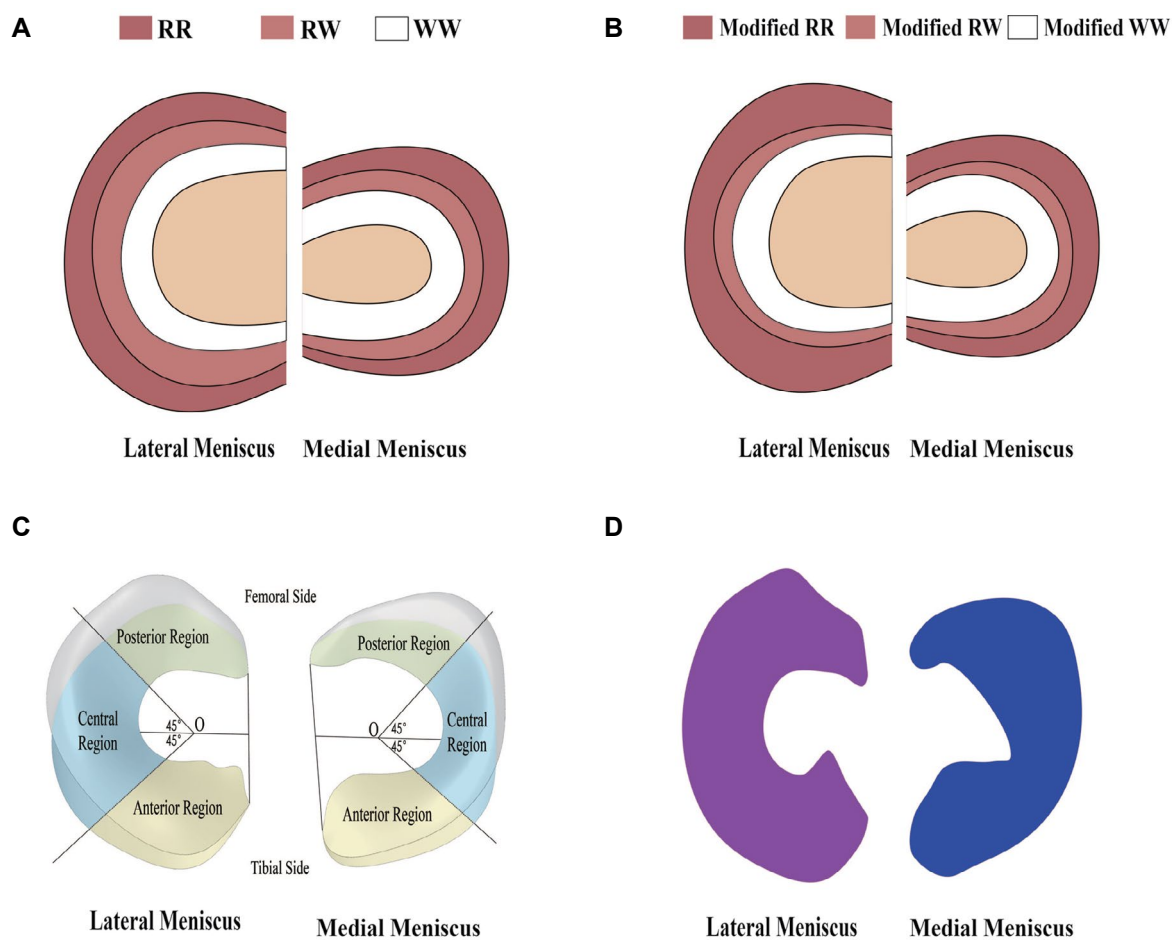


Fig.2: Schematic diagram of meniscus divisions in the mouse knee joint. **A.** Three-equal-width division. **B.** Modified division. **C.** Meniscus (anterior region; central region; posterior region). **D.** Meniscus (medial; lateral). RR; Red-red zone, RW; Red-white zone, and WW; White-white zone.

Statistical analysis

The collected meniscus fluorescence signals were statistically analysed using Microsoft Excel 2021 and StataSE 16.0, and plotted using GraphPad Prism 9 (GraphPad Software, USA). Normality of the data was tested using the Shapiro-Wilk test. The measurement data was Normally distributed data are written as mean \pm SD. Based on the normality and homogeneity of the variance, we used a single-factor analysis of variance (one-way ANOVA) to compare multiple groups ($n=3$) and Tukey's test for multiple comparisons. An unpaired t test was applied to compare the two groups ($n=2$, independent samples). All the tests were performed bilaterally. $P<0.05$ indicated statistical significance.

Results

Fluorescence count of traditional three-equal-width division of mouse meniscus

Supplementary Data show the fluorescence counts of the RR, RW, and WW zones according to the traditional three-equal-width division of the meniscus. The mean fluorescence counts were 1949 ± 444 (RR zone), 1528 ± 449 (RW zone), and 310 ± 110 (WW zone). The

fluorescence count in the RR zone was not significantly greater than the RW zone (one-way ANOVA-Tukey's test, $P>0.05$), whereas the fluorescence count in the RW zone was significantly greater than the WW zone (one-way ANOVA-Tukey's test, $P<0.05$). In addition, the fluorescence count in the RR zone was significantly higher than that in the WW zone (RR zone: 1949 ± 444 , WW zone: 310 ± 110 , one-way ANOVA-Tukey's test, $P<0.05$). The preceding data implied that there was no variation in the blood vessels between the RR and RW zones in the traditional division; therefore, the traditional division might not reflect the blood supply of the meniscus (Fig.3).

Fluorescence count of the modified division of mouse meniscus

The total fluorescence signal of each meniscus was counted and the width ratios of the modified RR, modified RW, and modified WW zones were calculated to distinguish variations in blood supply between adjacent zones in a 4:2:1 ratio (Tables S1-3, See Supplementary Online Information at www.celljournal.org). The mean fluorescence counts of all three mouse menisci in the modified zones were 2163 ± 570 (RR), 1081 ± 269 (RW), and 542 ± 138 (WW). There was a significant difference

in the fluorescence counts among the three zones (one-way ANOVA-Tukey's test, $P < 0.05$). Based on the data, the width ratios of the modified zones were $38 \pm 1\%$ (RR), $24 \pm 1\%$ (RW), and $38 \pm 2\%$ (WW). The width ratios of the modified RR and modified WW zones were wider than their ratio (33.3%) in the traditional division, whereas the modified RW zone was narrower than its original size. Therefore, 3D imaging and quantitative analysis showed that the modified division could better reflect the distribution of blood vessels in the mouse meniscus (Fig.4).

Fluorescence counts of anterior, central, and posterior regions of mouse meniscus

The fluorescence counts in the anterior, central, and posterior regions of the menisci are shown in the Tables S1-3 (See Supplementary Online Information at www.celljournal.org). The mean fluorescence counts for these regions were 1915 ± 550 (anterior), 567 ± 64 (central), and 1319 ± 375 (posterior). Based on the above data, the fluorescence intensity of the anterior region of the meniscus was greater than the posterior region, and the

signal intensity of the central region was lower than the posterior region. Both variables were statistically significant (one-way ANOVA-Tukey's test, $P < 0.05$). These results suggest that the number of blood vessels in the anterior region of the meniscus was greater than that in the posterior region, and the number of blood vessels in the posterior region was greater than that in the central region (Fig.5).

Fluorescence count of the medial and lateral meniscus in mouse

The fluorescence counts of the medial and lateral menisci of the mouse are shown in the Tables S1-3 (See Supplementary Online Information at www.celljournal.org). The mean fluorescence counts of the medial meniscus and lateral menisci of all three mice were 2516 ± 971 and 1287 ± 192 , respectively. The fluorescence count of the medial meniscus was significantly higher than the lateral meniscus (unpaired t test, $P < 0.05$). These results suggest that the number of blood vessels in the medial meniscus is greater than the lateral meniscus (Fig.6).

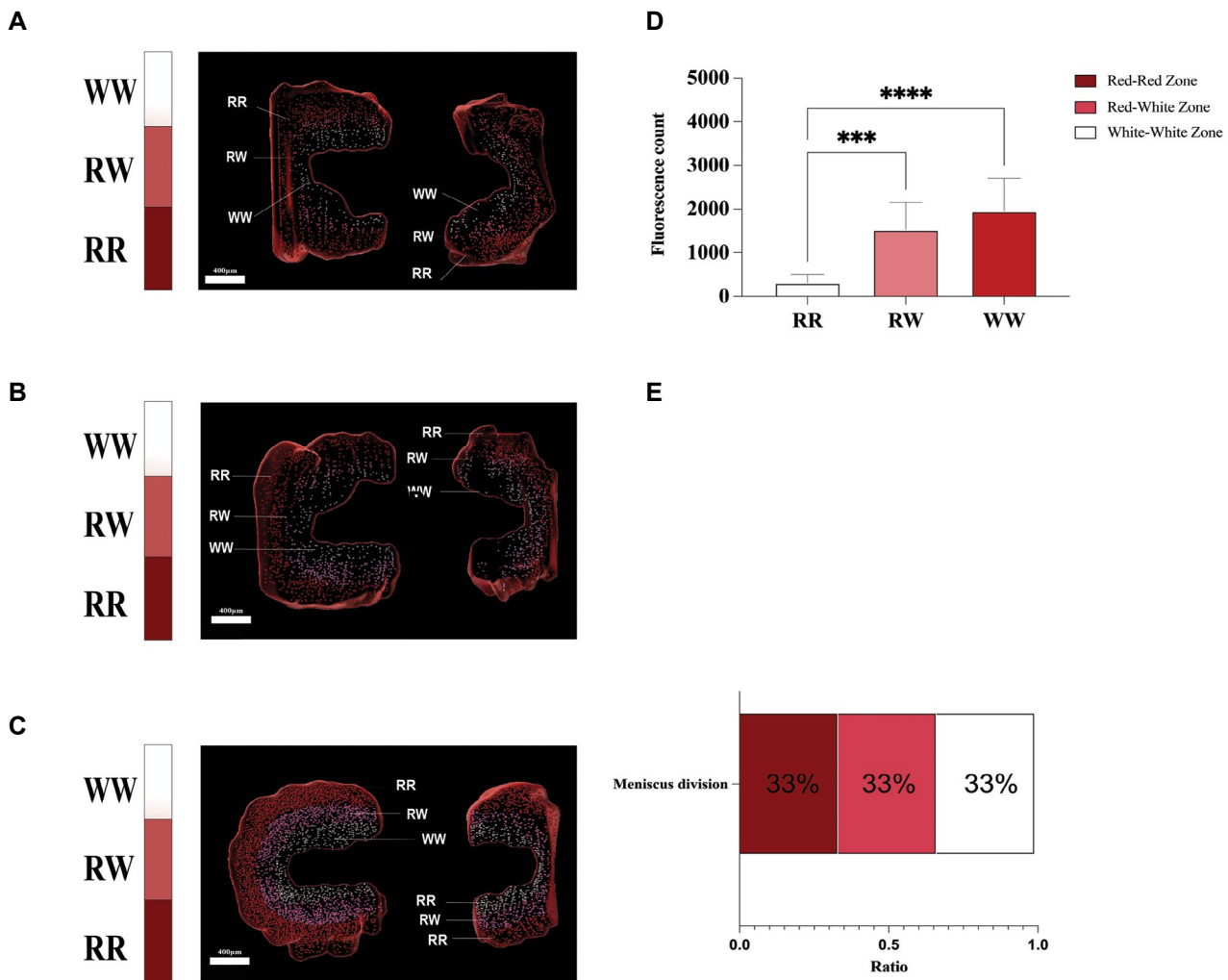


Fig.3: Three-equal-width division of the meniscus. **A-C.** Three-dimensional (3D) imaging of three-equal-width division of the meniscus (scale bar: 400 μ m). **D.** Statistical chart of fluorescence counts of the three-equal-width division. **E.** Statistical chart of the width of the three-equal-width division. ***, $P < 0.001$, ****, $P < 0.0001$, RR; Red-red zone, RW; Red-white zone, and WW; White-white zone.

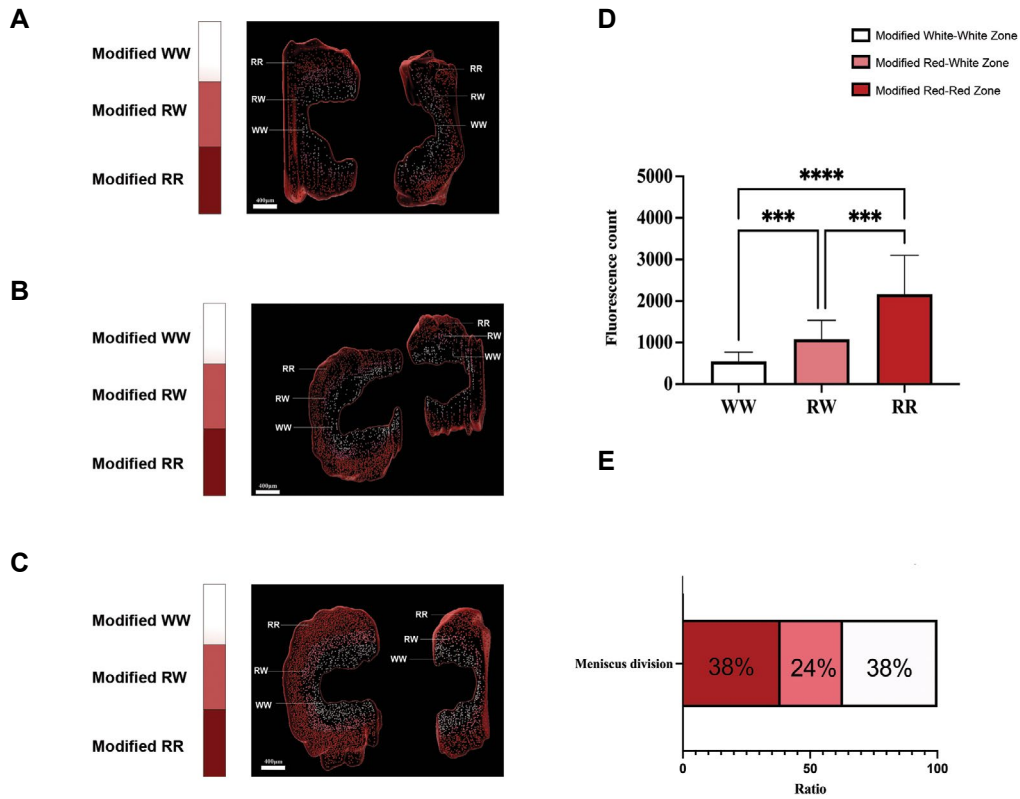


Fig.4: Modified division of the meniscus. **A-C.** Three-dimensional (3D) imaging of the modified division of the meniscus (scale bar: 400 μ m). **D.** Statistical chart shows the fluorescence count of the modified division. **E.** Statistical chart of the width ratio of the modified division. **, $P < 0.001$, ****, $P < 0.0001$, RR; Modified red-red zone, RW; Modified red-white zone, and WW; Modified white-white zone.

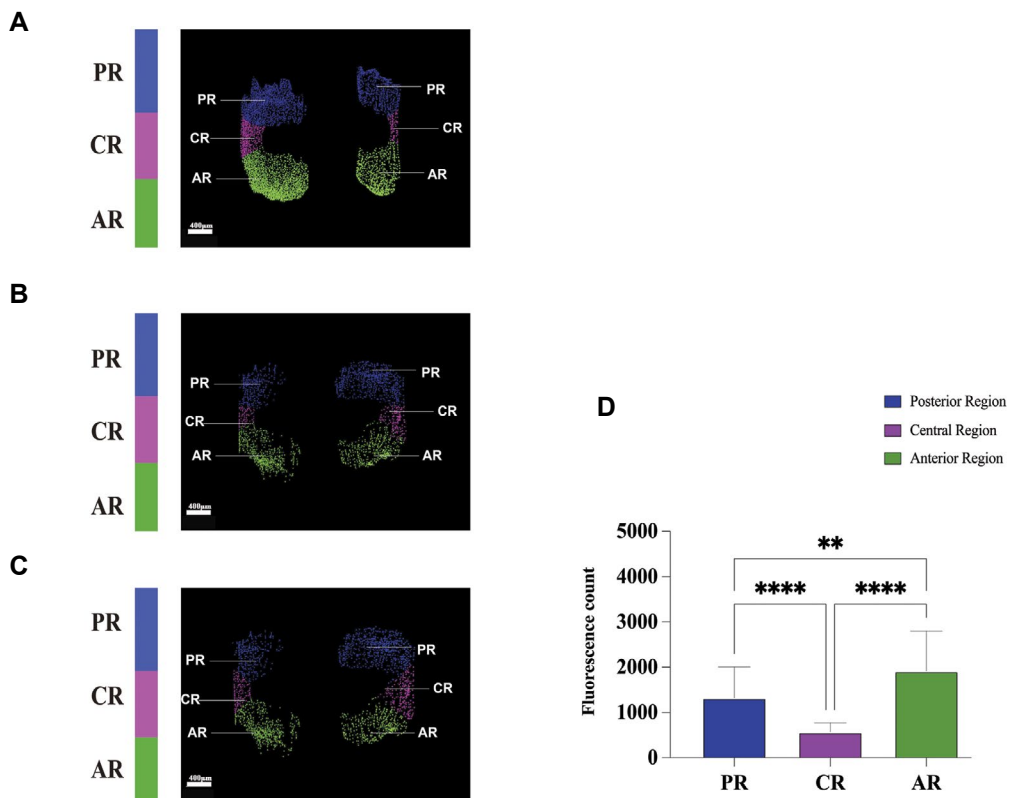


Fig.5: Blood supply of the anterior, central, and posterior regions of the meniscus. **A-C.** Three-dimensional (3D) imaging of blood supply to the anterior, central, and posterior regions of the meniscus (scale bar: 400 μ m). **D.** Statistical chart shows the blood supply of the anterior, central, and posterior regions of the meniscus. **, $P < 0.01$, ****, $P < 0.0001$, PR; Posterior region, CR; Central region, and AR; Anterior region.

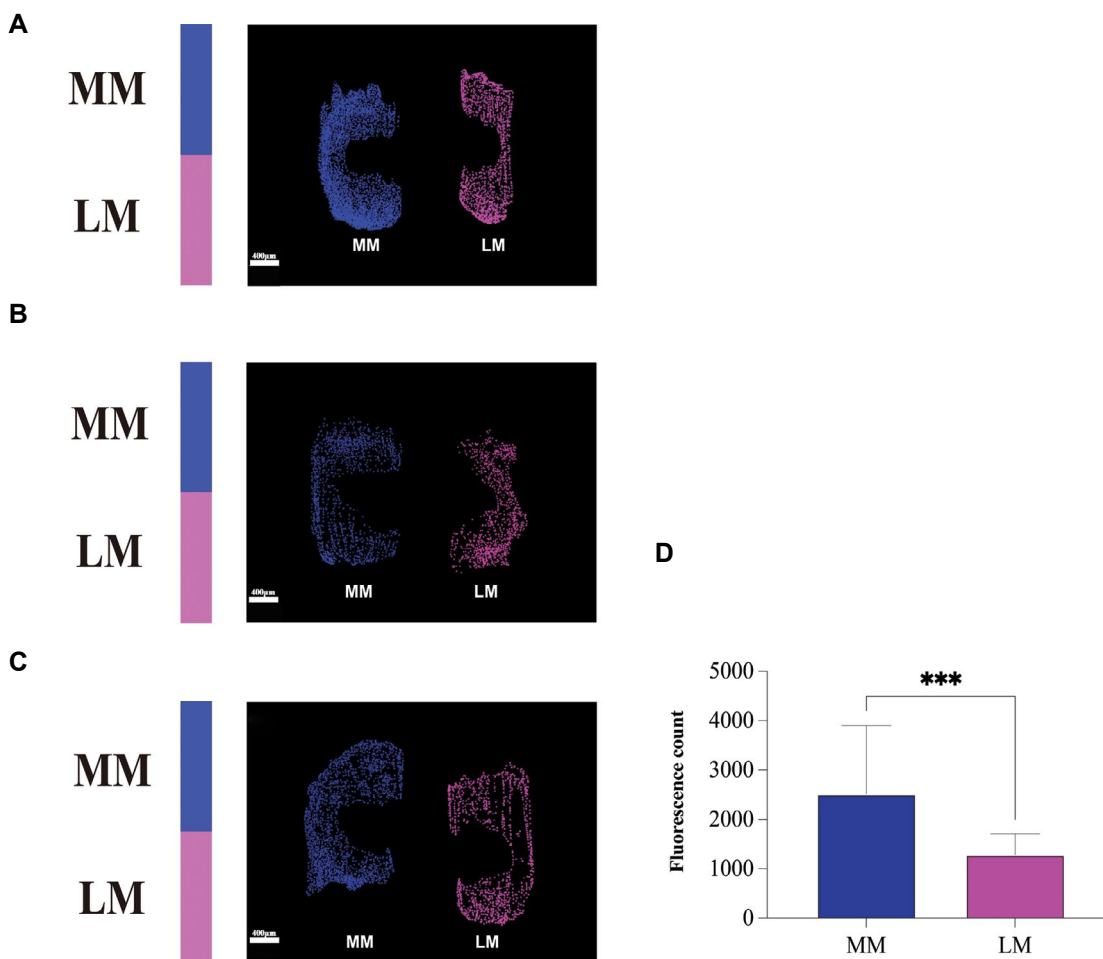


Fig.6: Blood supply of the medial and lateral meniscus. **A-C.** Three-dimensional (3D) reconstruction of the blood supply of the medial and lateral meniscus (scale bar: 400 μ m). **D.** Statistical chart shows the blood supply of the medial and lateral meniscus. ***; $P < 0.001$, MM; Medial meniscus, and LM; Lateral meniscus.

Discussion

Meniscal lesions caused by trauma and degeneration are among the most common types of knee joint injuries. Without prompt and proper treatment there is accelerated cartilage degeneration and loss, which leads to structural damage and dysfunction of the knee joint and, in severe cases, disability (26). Patients often require long-term treatment and perhaps face the possibility of knee arthroplasty once other treatments fail (27, 28). Basic research has demonstrated the crucial role of the meniscus in knee homeostasis (21). It has also shown that certain lesions have the potential to heal and thus can be repaired (12). Vascular supply is believed to be a key factor in enabling meniscal repair (29, 30). The main surgical treatment options that include arthroscopic meniscus repair and partial, subtotal, and total meniscectomies are based on lesion location, particularly in terms of vascularized or non-vascularized zones, on which healing depends (12, 17). According to the European Society for Sports Traumatology, Knee Surgery and Arthroscopy (ESSKA) meniscus consensus, longitudinal vertical tears caused by trauma in the RR zone are positive predictors of healing if the injury is treated properly in its initial stage and

should not be regarded as an absolute contraindication for meniscal repair (12, 17). Trauma in the RW zone was also an indication for higher success rate for meniscal repairs (31, 32). However, tears in the WW zone have inferior healing capability (12, 15). Therefore, the choice of nonoperative treatment or arthroscopic surgery should depend on the blood supply to the injury locations (22); hence, the blood supply to the meniscus deserves further study.

The vascularity of the menisci has been studied for nearly 100 years using various experimental methods such as haematoxylin and eosin staining (33), immunohistochemical staining (11), and ink staining (22). Distribution of vascularity appears to recede from the peripheral to the central zone (34, 35). Arnoczky and Warren (21) were the pioneers who used ink staining to provide a detailed description of microvasculature. Their study laid a solid foundation for understanding the anatomy to approach meniscal repair and originated the “RR,” “RW,” and “WW” terminology that depicted the perceived presence of blood supply in the meniscus. Their study showed that the absolute vascularized area, or RR zone, was approximately 3 mm in width near the

articular capsule; the absolute non-vascularized area (above 5 mm) was defined as the WW zone; and the relative vascularized area (5 mm apart) was defined as the RW zone (20). However, the blood supply to the meniscus warrants further study because ink staining may not sufficiently infiltrate the vascular endings (11). Day et al. (9) reported similar findings in an anatomical cadaveric study. This led to singular classification systems that divide the meniscus into several zones based on its blood supply (8, 10). Differentiation among the three-equal-width zones (RR, RW, and WW) is widely used, although the division cannot adequately depict the distribution of blood vessels in the meniscus. Based on the division and from the perspective of meniscus healing after an injury, it has been determined that one-third of the outer edge of the meniscus tends to heal well due to a sufficient blood supply, whereas one-third of the inner meniscus tends to heal slowly due to an inadequate blood supply (11, 36). These studies provided a general description of the blood supply to the meniscus and played a vital role in clinical guidance.

Intuitive quantitative research could reveal the law of blood supply of the meniscus that corresponds to division, and depict and assess the blood supply of the meniscus in another dimension as a supplement to the classical division. Researchers have used a light sheet microscope to photograph all of the tissue layers. Computer software synthesized the layered images to provide 3D structural imaging of the knee joint of the mouse. This study aimed to analyse the distribution of blood vessels in transgenic mice (Tie2-Gt (ROSA) 26Sor^{tm14}(CAG-tdTomato) Hze,002856). Therefore, 3D imaging combined with tissue clearing in transgenic mice can enable a precise study of the blood supply to the meniscus.

In the current study, we used 3D imaging after tissue clearing to conduct a quantitative analysis of the blood supply to the mouse meniscus. First, we observed that the blood vessels in the mouse meniscus gradually decreased from the outer edge to the inner edge. Second, the modified divisions were adjusted based on log transformation (4:2:1, $P < 0.05$). The width ratios of the modified division were $38 \pm 1\%$ (RR), $24 \pm 1\%$ (RW), and $38 \pm 2\%$ (WW), which more accurately displayed the distribution of blood vessels and provided more evidence for evaluating the meniscal blood supply. Therefore, clinical treatment based on blood supply illustrated by 3D imaging may be more suitable for patients. This can be used as a guide for the development of surgical strategies and conservative treatment. In contrast to a previous conclusion about the lack of a blood supply in the WW zone, Ribera et al. (37) reported the presence of vessels in this zone. In this study, a few signals were detected in the WW zone near the centre of the tibial plateau, which suggested that the vasculature from the peripheral zone penetrated the modified WW zone and that the modified WW zone might have healing potential (38). Finally, we observed the blood vessel distribution between the different structures of the meniscus. There were more blood vessels in the anterior

region of the meniscus compared to the posterior region, and more blood vessels in the posterior region than the central region, which suggested that the blood supply of the medial meniscus was better than the lateral meniscus, and injuries to the lateral meniscus were more difficult to heal than injuries to the medial meniscus. These findings confirmed the results of previous studies (22, 39).

This study has certain limitations. First, we conducted this experiment on mice because of the experimental limitations for tissue clearing and the restrictions for transgenic technology in humans. Therefore, it is necessary to extrapolate this model to the clinical situation with caution (21). Second, the presence of vascular endothelial cells may not necessarily indicate functional vascularization (40). Third, the sample size (six menisci) was small, which might result in bias. Fourth, considering that mice and humans have different leg forms and walking patterns, additional behavioural training should be implemented to maximize the similarity of the leg forms and walking patterns of mice to humans. Thus, instead of being a substitute for clinical experience, prudent orthopaedists should look upon these results as a foundation to predict a fundamental understanding of the meniscus in terms of its biological capabilities and vascular anatomy.

Conclusion

A combination of tissue clearing and 3D imaging technology in transgenic mice was used for quantitative analysis of the blood supply to the meniscus. In the modified division, the ratio of the RR zone to the WW zone was higher and that of the RW zone was lower compared to the traditional division. This study provided more precise insight into the blood supply to the mouse meniscus, and can provide a foundation for future research on the human meniscus.

Acknowledgments

This study was funded by The National Natural Science Foundation of China (81972129, 82072521, 82111530200), Sanming Project of Medicine in Shenzhen (SZSM201612078), Introduction Project of Clinical Medicine Expert Team for Suzhou (SZYJTD201714), Shanghai Talent Development Funding Scheme (2020080), Shanghai Committee of Science and Technology (22DZ2204900 and 23ZR1445700) and Shanghai Sailing Program (22YF1405200), Medical Engineering Joint Fund of Fudan University (YG2022-14), Science and Technology Innovation Project of General Administration of Sport of China (22KJCX010). The authors declare that they have no conflicts of interest.

Authors' Contributions

H.S., M.H., H.L.; Conceptualization and Methodology. Y.W., X.T.; Software and Validation. H.S., M.H., X.D.; Formal analysis. H.L.; Investigation. Y.W., X.T.; Resources. L.S., H.L.; Data Curation. H.S., S.F.; Writing

– Original Draft. M.H., H.L.; Writing – Review & Editing. H.S.; Visualization. Y.F.; Supervision. J.C., Y.L.; Project administration and Funding acquisition. All authors read and approved the final manuscript.

References

- Hutchinson ID, Moran CJ, Potter HG, Warren RF, Rodeo SA. Restoration of the meniscus: form and function. *Am J Sports Med.* 2014; 42(4): 987-998.
- Tanaka T, Fujii K, Kumagai Y. Comparison of biochemical characteristics of cultured fibrochondrocytes isolated from the inner and outer regions of human meniscus. *Knee Surg Sports Traumatol Arthrosc.* 1999; 7(2): 75-80.
- Chambers HG, Chambers RC. The natural history of meniscus tears. *J Pediatr Orthop.* 2019; 39 (6 Suppl 1): S53-S55.
- Hidaka C, Ibarra C, Hannafin JA, Torzilli PA, Quitariano M, Jen SS, et al. Formation of vascularized meniscal tissue by combining gene therapy with tissue engineering. *Tissue Eng.* 2002; 8(1): 93-105.
- Kobayashi K, Fujimoto E, Deie M, Sumen Y, Ikuta Y, Ochi M. Regional differences in the healing potential of the meniscus-an organ culture model to eliminate the influence of microvasculature and the synovium. *Knee.* 2004; 11(4): 271-278.
- Uchida R, Horibe S, Shiozaki Y, Shino K. All-inside suture repair for isolated radial tears at the midbody of the lateral meniscus. *Arthrosc Tech.* 2019; 8(12): e1451-e1456.
- Fox A J, Bedi A, Rodeo SA. The basic science of human knee menisci: structure, composition, and function. *Sports Health.* 2012; 4(4): 340-351.
- Fox AJ, Wanivenhaus F, Burge AJ, Warren RF, Rodeo SA. The human meniscus: a review of anatomy, function, injury, and advances in treatment. *Clin Anat.* 2015; 28(2): 269-287.
- Day B, Mackenzie WG, Shim SS, Leung G. The vascular and nerve supply of the human meniscus. *Arthroscopy.* 1985; 1(1): 58-62.
- Longo UG, Campi S, Romeo G, Spiezia F, Maffulli N, Denaro V. Biological strategies to enhance healing of the avascular area of the meniscus. *Stem Cells Int.* 2012; 2012: 528359.
- Michel PA, Domnick CJ, Raschke MJ, Hoffmann A, Kittl C, Herbst E, et al. Age-related changes in the microvascular density of the human meniscus. *Am J Sports Med.* 2021; 49(13): 3544-3550.
- Beaufils P, Pujol N. Management of traumatic meniscal tear and degenerative meniscal lesions. Save the meniscus. *Orthop Traumatol Surg Res.* 2017; 103(8S): S237-S244.
- Aman ZS, Dickens JF, Dekker TJ. Meniscal repair techniques for middle- and posterior-third tears. *Arthroscopy.* 2021; 37(3): 792-794.
- Lubowitz JH, Brand JC, Rossi MJ. Nonoperative management of degenerative meniscus tears is worth a try. *Arthroscopy.* 2020; 36(2): 327-328.
- Stärke C, Kopf S, Petersen W, Becker R. Meniscal repair. *Arthroscopy.* 2009; 25(9): 1033-1044.
- Hevesi M, Krych AJ, Kurzweil PR. Meniscus tear management: indications, technique, and outcomes. *Arthroscopy.* 2019; 35(9): 2542-2544.
- Kopf S, Beaufils P, Hirschmann MT, Rotigliano N, Ollivier M, Pereira H, et al. Management of traumatic meniscus tears: the 2019 ESSKA meniscus consensus. *Knee Surg Sports Traumatol Arthrosc.* 2020; 28(4): 1177-1194.
- Takata Y, Nakase J, Shimozaki K, Asai K, Tsuchiya H. Autologous adipose-derived stem cell sheet has meniscus regeneration-promoting effects in a rabbit model. *Arthroscopy.* 2020; 36(10): 2698-2707.
- Moatti A, Cai Y, Li C, Sattler T, Edwards L, Piedrahita J, et al. Three-dimensional imaging of intact porcine cochlea using tissue clearing and custom-built light-sheet microscopy. *Biomed Opt Express.* 2020; 11(11): 6181-6196.
- Arnoczky SP, Warren RF. Microvasculature of the human meniscus. *Am J Sports Med.* 1982; 10(2): 90-95.
- Arnoczky SP, Warren RF. The microvasculature of the meniscus and its response to injury. An experimental study in the dog. *Am J Sports Med.* 1983; 11(3): 131-141.
- Crawford MD, Hellwinkel JE, Aman Z, Akamefula R, Singleton JT, Bahney C, et al. Microvascular anatomy and intrinsic gene expression of menisci from young adults. *Am J Sports Med.* 2020; 48(13): 3147-3153.
- Luo W, Yi Y, Jing D, Zhang S, Men Y, Ge WP, et al. Investigation of postnatal craniofacial bone development with tissue clearing-based three-dimensional imaging. *Stem Cells Dev.* 2019; 28(19): 1310-1321.
- Broothaerts W, Cordeiro F, Corbisier P, Robouch P, Emons H. Log transformation of proficiency testing data on the content of genetically modified organisms in food and feed samples: is it justified? *Anal Bioanal Chem.* 2020; 412(5): 1129-1136.
- Feng C, Wang H, Lu N, Tu XM. Log transformation: application and interpretation in biomedical research. *Stat Med.* 2013; 32(2): 230-239.
- Beaufils P, Becker R, Kopf S, Englund M, Verdonk R, Ollivier M, et al. Surgical management of degenerative meniscus lesions: the 2016 ESSKA meniscus consensus. *Knee Surg Sports Traumatol Arthrosc.* 2017; 25(2): 335-346.
- Englund M, Roemer FW, Hayashi D, Crema MD, Guermazi A. Meniscus pathology, osteoarthritis, and the treatment controversy. *Nat Rev Rheumatol.* 2012; 8(7): 412-419.
- Krych AJ, Hevesi M, Leland DP, Stuart MJ. Meniscal root injuries. *J Am Acad Orthop Surg.* 2020; 28(12): 491-499.
- Cinque ME, DePhillipo NN, Moatshe G, Chahla J, Kennedy MI, Dornan GJ, et al. Clinical outcomes of inside-out meniscal repair according to anatomic zone of the meniscal tear. *Orthop J Sports Med.* 2019; 7(7): 2325967119860806.
- Jacob G, Shimomura K, Krych AJ, Nakamura N. The meniscus tear: a review of stem cell therapies. *Cells.* 2019; 9(1): 92.
- Barber-Westin SD, Noyes FR. Clinical healing rates of meniscus repairs of tears in the central-third (red-white) zone. *Arthroscopy.* 2014; 30(1): 134-146.
- Noyes FR, Barber-Westin SD. Repair of complex and avascular meniscal tears and meniscal transplantation. *J Bone Joint Surg Am.* 2010; 92(4): 1012-1029.
- Hennerbichler A, Moutos FT, Hennerbichler D, Weinberg JB, Guilak F. Repair response of the inner and outer regions of the porcine meniscus in vitro. *Am J Sports Med.* 2007; 35(5): 754-762.
- Clark CR, Ogden JA. Development of the menisci of the human knee joint. Morphological changes and their potential role in childhood meniscal injury. *J Bone Joint Surg Am.* 1983; 65(4): 538-547.
- Petersen W, Tillmann B. Age-related blood and lymph supply of the knee menisci. A cadaver study. *Acta Orthop Scand.* 1995; 66(4): 308-312.
- Williams LB, Adesida AB. Angiogenic approaches to meniscal healing. *Injury.* 2018; 49(3): 467-472.
- Ribera J, Pauta M, Melgar-Lesmes P, Córdoba B, Bosch A, Calvo M, et al. A small population of liver endothelial cells undergoes endothelial-to-mesenchymal transition in response to chronic liver injury. *Am J Physiol Gastrointest Liver Physiol.* 2017; 313(5): G492-G504.
- Chahla J, Papalamprou A, Chan V, Arabi Y, Salehi K, Nelson TJ, et al. Assessing the resident progenitor cell population and the vascularity of the adult human meniscus. *Arthroscopy.* 2021; 37(1): 252-265.
- Krych AJ, Bernard CD, Kennedy NI, Tagliero AJ, Camp CL, Levy BA, et al. Medial versus lateral meniscus root tears: is there a difference in injury presentation, treatment decisions, and surgical repair outcomes? *Arthroscopy.* 2020; 36(4): 1135-1141.
- Hohmann E. Editorial commentary: discovery: progenitor cells and endothelial cells are found in the white-white zone of the meniscus, but this does not mean that these tears heal or should be repaired. *Arthroscopy.* 2021; 37(1): 266-267.